Proceedings of the ASME 2014 Dynamic Systems and Control Conference
DSCC 2014
October 22-24, 2014, San Antonio, TX, USA

DSCC2014-5960

ITERATIVE FEEDFORWARD TUNING APPROACH AND EXPERIMENTAL VERIFICATION FOR NANO-PRECISION MOTION SYSTEMS

Frank Boeren[*], **Tom Oomen**
Department of Mechanical Engineering
Eindhoven University of Technology
Eindhoven, The Netherlands
Email: f.a.j.boeren@tue.nl, t.a.e.oomen@tue.nl

Dennis Bruijnen
Mechatronics Technologies
Philips Innovation Services
Eindhoven, the Netherlands
dennis.bruijnen@philips.com

ABSTRACT

Feedforward control can significantly improve the performance of industrial motion systems through compensation of the servo error induced by the reference signal. Recently, new feedforward tuning algorithms have been proposed that exploit measured data from previous tasks and a suitable feedforward parametrization to attain high servo performance. The aim of this paper is to formulate a design procedure for motion feedforward tuning. Experimental results on an industrial motion system illustrate the improvement in servo performance obtained by means of the proposed tuning procedure.

1 INTRODUCTION

Feedforward control is indispensable to attain high servo performance in industrial motion systems. Indeed, many applications to atomic force microscopes [1–3] and wafer scanners [4–6] have been reported where feedforward control leads to a significant improvement in servo performance. Relevant examples include model-based feedforward [3], [7], Iterative Learning Control (ILC) [8], and adaptive feedforward control [9].

ILC achieves superior servo performance for a single, specific reference. However, variations in the reference between consecutive tasks result in significant performance deterioration, see, e.g., [10]. This is clearly undesired in industrial motion systems, that inherently exhibit changes in the reference [6]. In contrast to ILC, model-based feedforward results in moderate servo performance for a class of reference signals. Furthermore, the application of adaptive feedforward to industrial motion systems is hampered by a persistence of excitation condition. This condition imposes unacceptable requirements on the reference signal during normal operation of the system.

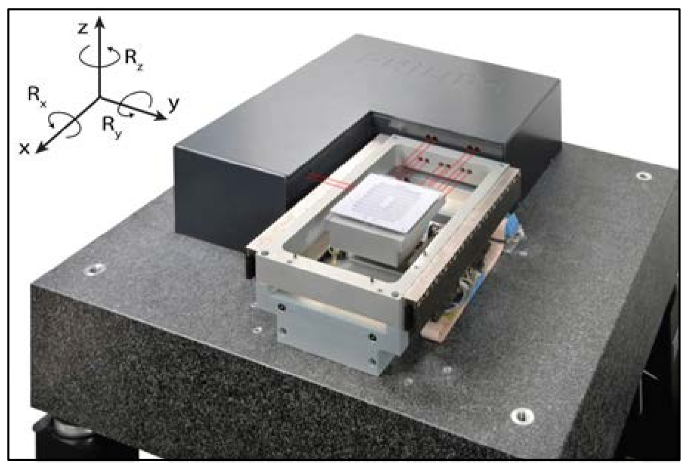

FIGURE 1: EXPERIMENTAL SETUP.

To facilitate implementation in industrial motion systems, two specifications are imposed on the feedforward controller: i) high servo performance, and ii) applicability to a class of reference signals. The iterative feedforward tuning approach proposed in [4] attains these specifications by combining a low-order, fixed structure feedforward parametrization with optimization of the corresponding parameters based on measured data. As such, this approach combines the advantages of model-

[*]Address all correspondence to this author.

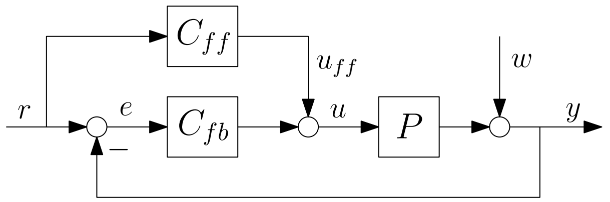

FIGURE 2: CONTROL CONFIGURATION.

based feedforward and ILC. That is, applicability to a class of reference signals is obtained by introducing a feedforward parametrization similar to model-based feedforward. High servo performance results from optimization of parameters based on measured data as in ILC. In addition, the need for an approximate model, as is common in ILC, is eliminated by exploiting concepts from Iterative Feedback Control (IFT) [11].

Recently, an iterative feedforward tuning procedure based on instrumental variables is proposed in [12] and [13], which leads to unbiased parameter estimates with optimal accuracy. To this end, concepts from closed-loop system identification are exploited in iterative feedforward tuning. A simulation study confirmed that this procedure leads to enhanced servo performance compared to pre-existing approaches. However, an experimental verification is not provided for an industrial motion system.

Although iterative feedforward tuning based on instrumental variables is conceptually promising, at present there is no design procedure and experimental validation presented for industrial motion systems. The contribution of this paper is twofold. First, a design procedure is proposed for motion feedforward tuning based on [13]. Second, an experimental verification is performed on the industrial motion system shown in Figure 1.

This paper is organized as follows. In Section 2, the goal of feedforward control is outlined for nano-precision motion systems. In Section 3, the proposed design procedure is provided for feedforward control. In Section 4, this design procedure is applied to the experimental setup in Figure 1, and experimental results are presented. Finally, conclusions are provided in Section 5.

Notation. For a vector x, $||x||_2^2 = x^T x$. The vector u is defined as $u = [u(1), u(2), \ldots, u(N)]^T \in \mathbb{R}^{N\times 1}$, where $u(t)$ is a measurement at time instant t for $t = 1, 2, \ldots, N$ with N the number of samples. Furthermore, the expected value $\mathbb{E}(x)$ is defined as $\mathbb{E}(x) = \int_{-\infty}^{\infty} x f(x) dx$, with probability density function $f(x)$.

2 FEEDFORWARD CONTROL GOAL

2.1 Experimental setup

The considered motion system is depicted in Figure 1. The actuation and measurement system, and the positioning stage are placed on a vibration isolation table to isolate the positioning system from external disturbances from the environment. The positioning stage is actuated and controlled in six motion degrees of freedom (DOF): three translations (x, y, and z) and three rotations (R_x, R_y and R_z). The system is equipped with six actuators to provide the required force. These actuators consist of linear magnetic motors with an added position offset such that an actuator can also generate a force in the perpendicular direction, see [14] for an explanation of the underlying principle.

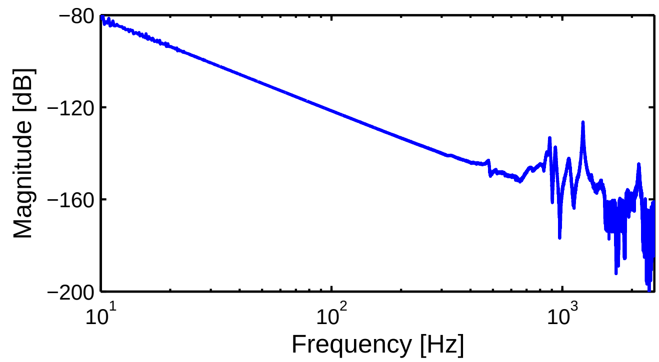

FIGURE 3: FREQUENCY RESPONSE FUNCTION OF THE SYSTEM P.

The measurement system consist of laser interferometers in conjunction with a mirror block, connected to the vibration isolation table and the positioning stage, respectively. This system enables high accuracy position measurements in all six motion DOFs. In particular, position measurements with subnanometer resolution are available for the translational DOFs x, y and z. Throughout, all systems and signals operate in discrete time with a sampling time of $T_s = 2 \times 10^{-4}$ s.

2.2 Control Configuration

Even though the experimental setup is an intrinsically multivariable system, the proposed design procedure for the feedforward controller is only applied to the x-direction of the system, i.e., the long stroke direction of the setup in Figure 1. A stabilizing feedback controller C_{fb}^{mimo} is determined for the multivariable system by means of sequential loopshaping, see, e.g., [15, Section 10.6]. By closing the control loops for the remaining 5 DOFs, i.e., y, z, R_x, R_y and R_z, a single-input, single output equivalent system P is obtained for the x-direction. It is furthermore assumed that P is a linear system. An identified frequency response function of the system P for the x-direction is depicted in Figure 3.

Consider the two degree-of-freedom control configuration as depicted in Figure 2 for the discrete-time, single-input single output, linear system P. The control configuration consists of a given stabilizing feedback controller C_{fb} and feedforward controller C_{ff}. The feedback controller C_{fb}, designed by means of manual tuning, attains a bandwidth (defined as the lowest frequency where $|C_{fb}P| = 1$) of 120 Hz. This bandwidth results in rejection of low-frequency disturbances, while having sufficient robustness against uncertainty in the resonances of P.

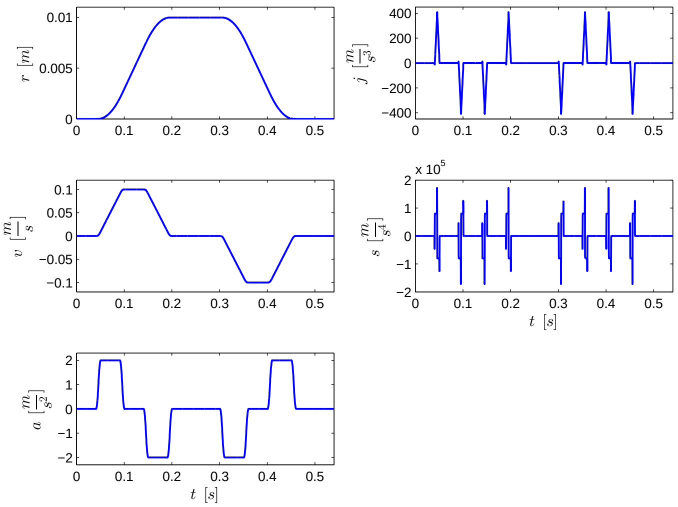

FIGURE 4: POSITION r, VELOCITY v, JERK j, AND SNAP s OF THE SERVO TASK.

Let r denote the known reference signal, w the unknown disturbance, u_{ff} the feedforward signal, y the output signal, and e the servo error. The (unknown) disturbance w is modeled as a stochastic process given by $w = H\varepsilon$, where H is monic and ε is zero mean normally distributed white noise with variance λ_ε^2. Hence, w and r are uncorrelated.

2.3 Feedforward Control Goal

The goal in feedforward control is to attain high performance by compensating for the servo error induced by the reference signal. To illustrate this statement, consider the servo error e in Figure 2 induced by the known reference signal r and unknown disturbance w given by

$$e = S(1 - PC_{ff})r - Sw, \tag{1}$$

with sensitivity function $S = (1 + PC_{fb})^{-1}$. From this expression it straightforwardly follows that the contribution of e induced by r is eliminated if $C_{ff} = P^{-1}$. This observation forms the basis of inversion-based feedforward control techniques. In the next section, a design procedure for feedforward control is provided that combines inversion-based feedforward with data-driven parameter estimation, aimed to achieve high servo performance.

3 DESIGN PROCEDURE FOR ITERATIVE FEEDFORWARD CONTROL

In this section, a design procedure is proposed for iterative feedforward control. In iterative feedforward control, measured data is exploited to update a fixed-structure feedforward controller C_{ff} after each task. For the considered industrial motion

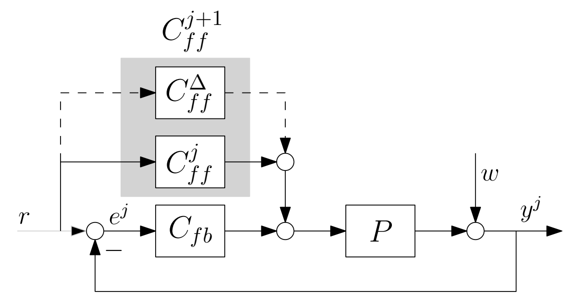

FIGURE 5: THE FEEDFORWARD CONTROLLER $C_{ff}^{j+1}(z)$ IS CONSTRUCTED BASED ON THE KNOWN REFERENCE r, AND MEASURED SIGNALS e^j AND y^j IN THE j^{th} TASK.

system, a sequence of finite time tasks, denoted by $j = 1, 2, \ldots$, is executed during normal operation. Note that the reference signal r is not necessarily identical in each task. A typical r conducted during a task is given in Figure 4 for the considered setup [16]. After each task, the feedforward controller implemented on the system during the j^{th} task, denoted $C_{ff}^j(z)$, is updated by $C_{ff}^\Delta(z)$. The data-driven optimization problem in iterative feedforward control is defined in Definition 1.

Definition 1. *Given measured signals e^j and y^j obtained during the j^{th} task of the system in Figure 2 with $C_{ff}^j(z)$ implemented. Then, as depicted in Figure 5,*

$$C_{ff}^{j+1}(z) = C_{ff}^j(z) + C_{ff}^\Delta(z), \tag{2}$$

where the update $C_{ff}^\Delta(z)$ based on e^j and y^j results from the optimization problem

$$C_{ff}^{\Delta,opt}(z) = \arg \min_{C_{ff}^\Delta \in \mathscr{C}} V(C_{ff}^\Delta), \tag{3}$$

with objective function $V(C_{ff}^\Delta)$ and feedforward controller parametrization $\mathscr{C}$.

The servo performance of the system in the $(j+1)^{\text{th}}$ task with $C_{ff}^{j+1}(z)$ is determined by the objective function $V(C_{ff}^\Delta)$ and parametrization $\mathscr{C}$. In Section 3.1, a suitable feedforward parametrization is introduced for nano-positioning motion systems. Then, in Section 3.2, an objective function $V(C_{ff}^\Delta)$ is introduced for iterative feedforward control based on instrumental variables.

3.1 Parametrization Feedforward Controller

In this section, a feedforward parametrization is introduced for nano-positioning systems. As presented in Section 2.3, the optimal feedforward controller is given by $C_{ff} = P^{-1}$. However, it is shown in [16] that C_{ff} only has to capture the low-frequency behavior of P^{-1} to eliminate the dominant component of the servo error induced by the reference r. This is explained by observing that the reference signal during a servo task has a dominant frequency content in the low-frequency range.

For the considered system in Figure 1, a typical reference r has a dominant frequency content below approximately 100 Hz. As a result, a feedforward parametrization is required for C_{ff} such that P^{-1} is approximated in the frequency range 0 - 130 Hz. Since the dynamical behavior of the system P is dominated by rigid-body dynamics in the considered frequency range, the parametrization for C_{ff} as proposed in [16] is adopted. The corresponding parametrization is defined in Definition 2.

Definition 2. *The feedforward controller $C_{ff}(z,\theta)$ is parametrized as*

$$C_{ff}(z,\theta) = \psi_v(z^{-1})\theta_v + \psi_a(z^{-1})\theta_a + \psi_j(z^{-1})\theta_j + \psi_s(z^{-1})\theta_s, \tag{4}$$

with basis functions

$$\Psi(z) = [\psi_v(z^{-1}),\ \psi_a(z^{-1}),\ \psi_j(z^{-1}),\ \psi_s(z^{-1})], \tag{5}$$

where

$$\begin{aligned} \psi_v(z^{-1}) &= \frac{1-z^{-1}}{T_s}, \\ \psi_a(z^{-1}) &= \frac{1-2z^{-1}+z^{-2}}{T_s^2}, \\ \psi_j(z^{-1}) &= \frac{1-3z^{-1}+3z^{-2}-z^{-3}}{T_s^3}, \\ \psi_s(z^{-1}) &= \frac{1-4z^{-1}+6z^{-2}-4z^{-3}+z^{-4}}{T_s^4}. \end{aligned} \tag{6}$$

and corresponding parameters $\theta = [\theta_v,\ \theta_a,\ \theta_j,\ \theta_s]^T \in \mathbb{R}^{n_\theta}$.

For motion systems with rigid-body dynamical behavior, it is desired that the feedforward signal u_{ff} is equal to zero if the system is in stand-still. In the parametrization of $C_{ff}(z,\theta)$ in Definition 2, this condition is enforced since it holds that

$$C_{ff}(z,\theta)|_{z=1} = 0, \tag{7}$$

i.e., the static gain of $C_{ff}(z,\theta)$ is equal to zero. Hence, the parametrization in Definition 2 is applicable to motion systems with rigid-body dynamical behavior.

Remark 1. *The parametrization in Definition 2 is a generalization of a FIR basis, and is as such applicable to a general class of systems.*

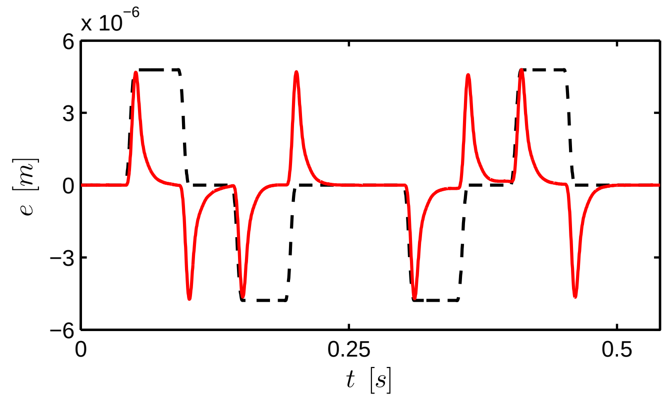

FIGURE 6: TUNING OF A FEEDFORWARD CONTROLLER FOR A MOTION SYSTEM - DECORRELATE THE ACCELERATION PROFILE a (DASHED BLACK) AND MEASURED SERVO ERROR e (RED).

The feedforward controller $C_{ff}(z,\theta)$ in Definition 2 has three key attributes. First, the parametrization is linear in θ. Therefore, if $V(C_{ff}^{\Delta})$ in Definition 1 is a quadratic objective function in θ, there is an analytic solution for θ. Second, as shown in [12, Theorem 4], the parametrization for C_{ff} in Definition 2 enables the use of recursive estimates of the parameters θ. That is, expression (2) in Definition 1 is equivalent to

$$\begin{aligned} C_{ff}^{j+1}(z,\theta^{j+1}) &= C_{ff}^{j}(z,\theta^{j}) + C_{ff}^{\Delta}(z,\hat{\theta}^{\Delta}) \\ &= \Psi(z)\left(\theta^{j}+\hat{\theta}^{\Delta}\right), \end{aligned} \tag{8}$$

where the update $\hat{\theta}^{\Delta}$ is computed based on the measured signals e^j and y^j during the j^{th} task. Third, since all poles of $C_{ff}^{j+1}(z,\theta)$ are located in the origin of the complex plane, stability of C_{ff}^{j+1} is guaranteed. As a result, implementation of $C_{ff}^{j+1}(z,\theta^{j+1})$ on the system is not hampering internal stability of the system in Figure 2.

The basis functions in Definition 2 facilitate a physical interpretation of the corresponding parameters. For example, θ_a represents the mass of the system. To illustrate this statement, observe that the feedforward signal $u_{ff} = C_{ff}(z,\theta)r$ corresponding to the parametrization for C_{ff} in Definition 2 is given by

$$u_{ff} = \theta_v v + \theta_a a + \theta_j j + \theta_s s, \tag{9}$$

where $v = \psi_v(z^{-1})r$, $a = \psi_a(z^{-1})r$, $j = \psi_j(z^{-1})r$ and $s = \psi_s(z^{-1})r$ correspond to respectively velocity, acceleration, jerk and snap, i.e., the 1^{st}, 2^{nd}, 3^{th} and 4^{th} derivative of r, with corresponding parameters θ_v, θ_a, θ_j, θ_s.

Remark 2. *Initial parameters θ^0 are determined using information about the system, if available, or otherwise set to zero. For example, the mass of a motion system is typically accurately known and can therefore be used as initial value for θ_a.*

In the next section, a data-driven optimization problem is provided to determine θ_v, θ_a, θ_j and θ_s based on measured data obtained during iterative tasks.

3.2 Data-Driven Optimization Algorithm

In this section, a data-driven optimization problem is defined to estimate the parameters $\hat{\theta}^\Delta$ based on measured data obtained in the j^{th} task. First, an objective function $V(C_{ff}^\Delta)$ is introduced for iterative feedforward control based on instrumental variables. Second, by exploiting concepts from Iterative Feedback Tuning [11], it is shown that $\hat{\theta}^\Delta$ can be estimated based on measured data only, i.e., without modelling S and P.

For the feedforward parametrization introduced in Definition 2, the optimization problem in Definition 1 is recast to

$$\hat{\theta}^\Delta = \arg\min_{\theta^\Delta} V(\theta^\Delta), \tag{10}$$

and $C_{ff}^{j+1}(z,\theta^{j+1})$ is determined according to (8). In this paper, the objective function $V(\theta^\Delta)$ is adopted from iterative feedforward control based on instrumental variables, see [12].

The instrumental variable framework for feedforward control essentially aims to decorrelate e and r. For example, consider acceleration feedforward $\theta_a a$. The normalized acceleration profile a and measured error e^j are depicted in Figure 6 for the considered motion system, where $C_{ff}^j = 0$ and r as in Figure 4. Clearly, a and e^j are correlated. The optimal value for θ_a in an instrumental variable framework is such that the predicted error

$$\hat{e}^{j+1}(\theta_a) = e^j - SP\theta_a a, \tag{11}$$

and a are uncorrelated. Likewise, the optimal values for θ_v, θ_j and θ_s are obtained if $\hat{e}^{j+1}$, and v, j and s are uncorrelated, respectively. The corresponding objective function $V(\theta^\Delta)$ is defined in Definition 3.

Definition 3. *The objective function $V(\theta^\Delta)$ in* (10) *is given by*

$$V(\theta^\Delta) = \left|\left|Z^T L(z)\hat{e}^{j+1}(\theta^\Delta)\right|\right|_W^2, \tag{12}$$

where $Z \in \mathbb{R}^{N\times n_z}$ are instrumental variables, W is a positive-definite weighting matrix, $n_z \geq n_\theta$, and $L(z)$ is a prefilter. The predicted error $\hat{e}^{j+1}(\theta^\Delta)$ for the $(j+1)^{th}$ task is given by

$$\hat{e}^{j+1}(\theta^\Delta) = e^j - SP\Psi\theta^\Delta r. \tag{13}$$

A key attribute of iterative feedforward control approaches is that $\hat{\theta}^\Delta$ is estimated without constructing non-parametric or parametric models of P and SP, see, e.g., [12]. This straightforwardly implies that SP should be eliminated in (13). Therefore, the following result from [4] is used

$$\mathbb{E}\left\{(C_{fb}+C_{ff}^j)^{-1}y^j\right\} = SPr, \tag{14}$$

which is based on the assumption that w is given by $w = H\varepsilon$, and ε is normally distributed white noise with zero mean and variance λ_ε^2. By exploiting the commutative property of single-input, single-output systems and (14), the predicted error in the $(j+1)^{\text{th}}$ task given by (13) becomes

$$\hat{e}^{j+1}(\theta^\Delta) = e^j - \Phi^j\theta^\Delta, \tag{15}$$

where $\Phi^j = \Psi(C_{fb}+C_{ff}^j)^{-1}y^j$. As a result, the predicted error $\hat{e}^{j+1}(\theta^\Delta)$ is determined without modeling S and P. This intermediate step is essential to estimate θ^Δ based on measured data only. To illustrate this statement, consider the basic instrumental variable approach, i.e., $Z \in \mathbb{R}^{N\times n_\theta}$, $n_z = n_\theta$, $W = I$ and $L = 1$ [17, Chapter 3]. Then, $\hat{\theta}^\Delta$ based on the optimization problem (10) with objective function $V(\theta^\Delta)$ in Definition 3 result from the set of equations

$$Z^T\left[e^j - \Phi^j\hat{\theta}^\Delta\right] = 0, \tag{16}$$

where the solution to (16) is given by

$$\hat{\theta}^\Delta = (Z^T\Phi^j)^{-1}Z^Te^j. \tag{17}$$

In (17), Φ^j and e^j are based on measured data from the j^{th} task only, while the instruments Z are design variables. Hence, if Z is constructed without modeling S and P, the optimization problem (10) is data-driven. In the next section, a design for the instrumental variables Z is proposed.

Remark 3. *The preview-based stable inversion approach in [18] is used to compute $(C_{fb}+C_{ff}^j)^{-1}y^j$ for unstable $(C_{fb}+C_{ff}^j)^{-1}$.*

3.3 Design of Instrumental Variables

In this section, a design for the instrumental variables Z is presented that i) is constructed based on measured data only, ii) results in unbiased estimates of $\hat{\theta}^\Delta$, and iii) attains optimal accuracy. To this end, the results derived in [12] and [13] are exploited in the design of Z.

In [12, Theorem 3] it is shown that unbiased estimates, i.e., $\mathbb{E}\hat{\theta}^{\Delta} = \theta_0^{\Delta}$ where θ_0^{Δ} are the true parameters, are obtained if Z and w are uncorrelated. In fact, this is the key motivation to prefer iterative feedforward control based on instrumental variables to least-squares techniques, which result in biased estimates in the presence of w. To achieve that Z and w are uncorrelated, the known reference r is used in Z. The remaining design freedom in Z is exploited in [13] to determine instruments Z that minimize the variance of the parameters $\hat{\theta}^{\Delta}$.

In [13], expressions are derived for the instrumental variables Z, weighting matrix W and prefilter $L(z)$ that result in optimal accuracy. For the basic instrumental variable approach, the optimal instrumental variables are given by

$$Z^{\text{opt}} = \Psi(C_{fb} + C_{ff}^j) y_r^j, \tag{18}$$

where $y_r^j = SP(C_{fb} + C_{ff}^j) r$ is the reference-induced contribution to the output signal y^j in the j^{th} task. Clearly, a model of SP is required to determine y_r^j. As explained in Section 3.2, this is undesired in iterative feedforward control.

To avoid modeling of SP, an approximate implementation of the optimal instrumental variables Z^{opt} is proposed in [13] that leads to optimal accuracy. The proposed instrumental variables are given by

$$Z^{\text{prop}} = \Psi(C_{fb} + C_{ff}^j)^{-1} r, \tag{19}$$

and require a bootstrap procedure to iteratively refine the instruments, similar to [19, Section 5] for closed-loop identification. In the next section, the bootstrap procedure is included in a procedure to determine $C_{ff}^{j+1}(z, \theta^{j+1})$ based on measured signals in the j^{th} task.

3.4 Procedure for Iterative Feedforward Control

In this section, a design procedure is proposed for iterative feedforward control based on instrumental variables. This design procedure, as provided in Procedure 1, combines i) the parametrization for C_{ff} derived in Section 3.1, ii) the data-driven optimization algorithm proposed in Section 3.2, and iii) the bootstrap method to refine Z as elaborated in Section 3.3.

Procedure 1. *Estimation of $\hat{\theta}^{\Delta}$ after j^{th} task*

1. *Measure e^j and y^j in the j^{th} task.*
2. *Construct $\Phi^j = \Psi(C_{fb} + C_{ff}^j)^{-1} y^j$.*
3. *Bootstrap procedure for $i = 1, 2, \ldots, M$:*
   a) *Set $\hat{\theta}^{\Delta}_{<i>}$ equal to zero.*
   b) *Construct $C^{j+1}_{ff,<i>} = \Psi(\theta^j + \hat{\theta}^{\Delta}_{<i>})$.*
   c) *Construct instrumental variables $Z_{<i>} = \Psi(C_{fb} + C^j_{ff,<i>})^{-1} r$.*
   d) *solve $\hat{\theta}^{\Delta}_{<i>} = (Z^T_{<i>} \Phi^j)^{-1} Z^T_{<i>} e^j$.*
   e) *Set $i \to i+1$ and repeat from Step 3.b until a stopping criterion is met.*
4. *Set $\hat{\theta}^{\Delta} = \hat{\theta}^{\Delta}_{<i>}$.*
5. *Construct $C_{ff}^{j+1} = \Psi(\theta^j + \hat{\theta}^{\Delta})$.*
6. *Set $j \to j+1$ and go to Step 1.*

The bootstrap procedure in Step 3 of Procedure 1 alternates between improving the instrumental variable Z and estimating the parameters $\hat{\theta}^{\Delta}$. In the next section, Procedure 1 is employed to determine a feedforward controller C_{ff}^{j+1} for the industrial motion system depicted in Figure 1.

4 APPLICATION TO THE EXPERIMENTAL SETUP

In this section, Procedure 1 is employed to determine a feedforward controller C_{ff} which attains high servo performance when implemented on the experimental setup in Figure 1. Therefore, 5 finite time tasks are performed, where the reference signal, as depicted in Figure 4, is identical in each task. For the first task, the initial feedforward controller C_{ff}^0 has initial parameters $\theta^0 = [0,\ 0,\ 0,\ 0]^T \in \mathbb{R}^{n_\theta}$. Subsequently, the steps outlined in Procedure 1 are followed to iteratively update the feedforward controller.

The measured error signal e^j in the 1st, 2nd and 3th task are depicted in Figure 7, while the corresponding cumulative power spectrum is provided in Figure 8. In addition, the two-norm of the error signal as a function of tasks is shown in Figure 9. The following observations are made:

1) Feedforward control significantly reduces the servo error for the considered system. A reduction in peak value and two-norm of the measured error signal of approximately 97 % is obtained by applying Procedure 1 to the considered system.
2) Figure 9 shows that two tasks are required to converge. If the closed-loop system in Figure 2 satisfied the assumption given in Section 2, only a single task is sufficient to converge. However, the system to-be-controlled is not fully described by the linear system P, and the disturbance w contains repetitive and deterministic components. This motivates the use of iterative tasks to update the feedforward controller, since iterative tasks are useful to minimize the influence of iteration-invariant disturbances, nonlinearities and measurement noise on the servo performance obtained, see, e.g., [20].
3) Figure 7 and Figure 8 indicate that the low-frequency contribution up to approximately 10 Hz is not compensated for by the feedforward controller, despite it is repetitive. This

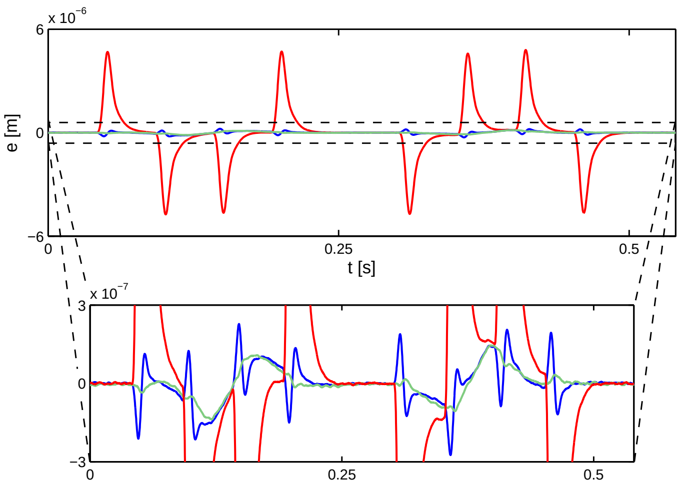

FIGURE 7: ERROR SIGNAL IN 1^{th} (RED), 2^{nd} (BLUE) AND 3^{th} (GREEN) TASK. A REDUCTION OF 97 % IN THE PEAK VALUE OF THE SERVO ERROR IS OBTAINED BY USING ITERATIVE FEEDFORWARD CONTROL.

implies that the dynamical behavior of the system is not captured by the basis functions in this frequency range. This repetitive error is contributed to cable slab between the fixed world and the (moving) positioning stage, which acts as a low-frequency disturbance on the system and is not included in the selected basis functions.

4) Figure 7 shows that the error in 3^{th} task is not identical during forward and backward movement. Again, this is contributed to cable slab, which has a preferred direction.

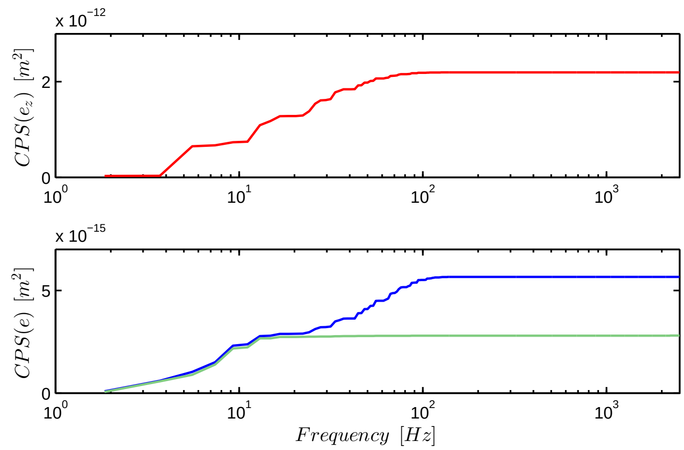

FIGURE 8: CUMULATIVE POWER SPECTRUM OF THE ERROR SIGNAL IN THE 1^{th} (RED), 2^{nd} (BLUE) AND 3^{th} (GREEN) TASK.

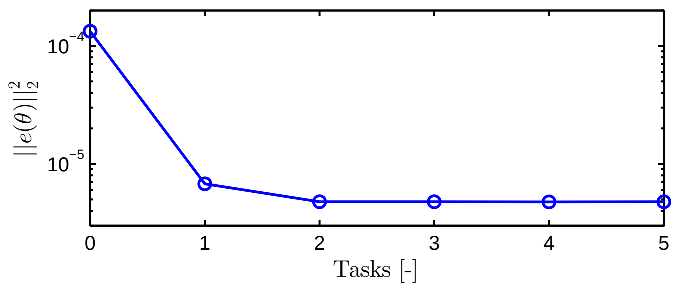

FIGURE 9: TWO-NORM OF THE MEASURED ERROR SIGNAL AS A FUNCTION OF TASKS.

5 CONCLUSIONS

Feedforward control is essential to attain high servo performance in industrial motion systems. In this paper, a design procedure is proposed to determine a fixed-structure feedforward controller based on measured data in iterative tasks. Therefore, theoretical results derived in [12] and [13] are exploited and recast in a design procedure. This procedure is successfully applied to an industrial motion system. Experimental results confirm that a significant improvement in servo performance is obtained for the considered system.

The proposed approach can be extended to other optimization problems in a closed-loop configuration. Ongoing research focuses on extensions to recursive estimation which exploit measured data from multiple tasks including stochastic approximation, input shaping [21], rational feedforward [22], multivariable systems, inferential control and positioning-varying effects [23]. For the considered motion system in Figure 1, improved performance can be obtained by including cable slap between the fixed world and the (moving) positioning stage in the set of basis functions.

ACKNOWLEDGMENT

The authors acknowledge Leon van Breugel and Maarten Steinbuch for their contribution to the early stages of this work. This research is supported by Philips Innovation Services and by the Innovational Research Incentives Scheme under the VENI grant Precision Motion: Beyond the Nanometer (no. 13073) awarded by NWO (The Netherlands Organisation for Scientific Research) and STW (Dutch Science Foundation).

REFERENCES

[1] Clayton, G. M., Tien, S., Leang, K. K., Zou, Q., and Devasia, S., 2009. "A review of feedforward control approaches in nanopositioning for high-speed SPM". *Journal of Dynamic Systems, Measurement, and Control,* **131**(6), pp. 0611011 – 061101–19.

[2] Tien, S., Zou, Q., and Devasia, S., 2005. "Iterative control of dynamics-coupling-caused errors in piezoscanners during high-speed AFM operation". *IEEE Transactions on Control Systems Technology,* **13**(6), pp. 921–931.

[3] Butterworth, J., Pao, L., and Abramovitch, D., 2012. "Analysis and comparison of three discrete-time feedforward model-inverse control techniques for nonminimum-phase systems". *Mechatronics,* **22**, pp. 577–587.

[4] van der Meulen, S., Tousain, R., and Bosgra, O., 2008. "Fixed structure feedforward controller design exploiting iterative trials: Application to a wafer stage and a desktop printer". *Journal of Dynamic Systems, Measurement, and Control,* **130**(5), pp. 0510061–05100616.

[5] Stearns, H., Yu, S., Fine, B., Mishra, S., and Tomizuka, M., 2008. "A comparative study of feedforward tuning methods for wafer scanning systems". In ASME Dynamic Systems and Control Conference, Michigan, USA.

[6] Oomen, T., van Herpen, R., Quist, S., van de Wal, M., Bosgra, O., and Steinbuch, M., 2014. "Connecting system identification and robust control for next-generation motion control of a wafer stage". *IEEE Transactions on Control Systems Technology,* **22**(1), pp. 102–118.

[7] Zhong, H., Pao, L. Y., and de Callafon, R. A., 2012. "Feedforward control for disturbance rejection: Model matching and other methods". In Proceedings of the Chinese Conference on Decision and Control, Taiyuan, China, pp. 3525–3533.

[8] Bristow, D., Tharayil, M., and Alleyne, A., 2006. "A survey of iterative learning control". *IEEE Control Systems Magazine,* **26**(3), pp. 96–114.

[9] Landau, I. D., Lozano, R., MSaad, M., and Karimi, A., 2011. *Adaptive Control: Algorithms, Analysis and Applications*, 2 ed. Communications and Control Engineering. Springer-Verlag, London, United Kingdom.

[10] Hoelzle, D. J., Alleyne, A. G., and Johnson, A. J. W., 2011. "Basis task approach to iterative learning control with applications to micro-robotic deposition". *IEEE Transactions on Control Systems Technology,* **19**(5), pp. 1138–1148.

[11] Hjalmarsson, H., Gevers, M., Gunnarsson, S., and Lequin, O., 1998. "Iterative feedback tuning: theory and applications". *IEEE Control Systems,* **18**(4), pp. 26–41.

[12] Boeren, F., and Oomen, T., 2013. "Iterative feedforward control: a closed-loop identification problem and a solution". In Proceedings of the 52st Conference on Decision and Control, Firenze, Italy, pp. 6694–6699.

[13] Boeren, F., Oomen, T., and Steinbuch, M., 2014. "Accuracy aspects in motion feedforward tuning". In Proceedings of the American Control Conference, Portland, OR, USA, pp 2178–2183.

[14] Angelis, G., and Biloen, D., 2008. Ironless magnetic linear motors having levitating and transversal force capacities, Patent, US 2008/0246348.

[15] Skogestad, S., and Postlethwaite, I., 2005. *Multivariable Feedback Control: Analysis and Design*, second ed. John Wiley & Sons, West Sussex, United Kingdom.

[16] Lambrechts, P., Boerlage, M., and Steinbuch, M., 2005. "Trajectory planning and feedforward design for electromechanical motion systems". *Control Engineering Practice,* **13**(2), pp. 145–157.

[17] Söderström, T., and Stoica, P., 1983. *Instrumental Variable Methods for System Identification*. Springer-Verlag, Berlin, Germany, volume 57 of Lecture Notes in Control and Information Sciences.

[18] Zou, Q., 2009. "Optimal preview-based stable-inversion for output tracking of nonminimum-phase linear systems". *Automatica,* **45**(1), pp. 230–237.

[19] Gilson, M., and Van den Hof, P., 2005. "Instrumental variable methods for closed-loop system identification". *Automatica,* **41**, pp. 241–249.

[20] Gunnarsson, S., and Norrlöf, M., 2006. "On the disturbance properties of high order iterative learning control algorithms". *Automatica,* **42**(11), pp. 2031–2034.

[21] Boeren, F., Bruijnen, D., van Dijk, N., and Oomen, T., 2014. "Joint input shaping and feedforward for point-to-point motion: Automated tuning for an industrial nanopositioning system". *Mechatronics*.

[22] Bolder, J., Oomen, T., and Steinbuch, M., 2014. "Rational basis functions in iterative learning control - with experimental verification on a motion system". *IEEE Transactions on Control Systems Technology*.

[23] Groot Wassink, M., van de Wal, M., Scherer, C., and Bosgra, O., 2005. "LPV control for a wafer stage: beyond the theoretical solution". *Control Engineering Practice,* **13**(2), pp. 231–245.